Morphological Classification: Application to Cardiac MRI of Tetralogy of Fallot

Dong Hye Ye[1], Harold Litt[2], Christos Davatzikos[1], and Kilian M. Pohl[1]

[1] SBIA, University of Pennsylvania, Philadelphia, USA
[2] Cardiovascular Imaging Section, University of Pennsylvania, Philadelphia, USA

Abstract. This paper presents an image-based classification method, and applies it to classification of cardiac MRI scans of individuals with Tetralogy of Fallot (TOF). Clinicians frequently diagnose cardiac disease by measuring the ventricular volumes from cardiac MRI scans. Interrater variability is a common issue with these measurements. We address this issue by proposing a fully automatic approach for detecting structural changes in the heart. We first extract morphological features of each subject by registering cardiac MRI scans to a template. We then reduce the size of the features via a nonlinear manifold learning technique. These low dimensional features are then fed into nonlinear support vector machine classifier identifying if the subject of the scan is effected by the disease. We apply our approach to MRI scans of 12 normal controls and 22 TOF patients. Experimental result demonstrates that the method can correctly determine whether subject is normal control or TOF with 91% accuracy.

Keywords: Tetralogy of Fallot, Morphological classification, Manifold learning, Computational anatomy.

1 Introduction

Cardiac MRI has become essential for pre- and post-operative management of tetralogy of Fallot patients [1]. This non-invasive technique can yield detailed 3D anatomical images of the beating heart with constant image quality through time. Clinicians use cardiac MRI to perform volumetric measurements of anatomical structures, such as left/right ventricular end-diastolic/end-systolic volumes, mass, stroke volumes, and ejections fractions. However, these measurements are often not sensitive enough to detect certain cardiac disease as they do not fully utilize the rich information provided by cardiac MRI. In addition, clinicians often find it difficult to produce reliable prediction of disease progression due to the high inter- and intra-rater variability associated with these measurements. We address this issue in this paper by suggesting an alternative approach for accurately detecting heart disease.

Our approach is based on a popular concept in the vision community, where high-dimensional features are extracted from the images and then fed into a classifier. The classifier automatically labels the image, which in our case corresponds to differentiating cardiac MRIs of patients effected by a certain disease

D.N. Metaxas and L. Axel (Eds.): FIMH 2011, LNCS 6666, pp. 180–187, 2011.

from healthy individuals. One issue with this type of analysis with respect to cardiac MRI is the relative low sample size in comparison to the high dimensionality of the image features. The number of training subjects impacted by a disease is often limited to hundreds while the number of voxels in a medical scan is typically more than a million. The community has addressed this issue by mapping the high-dimensional features into a lower dimensional space.

Principal component analysis (PCA) performs a linear mapping of the high dimensional features to a lower dimensional space such that the variance of the features in the lower dimensional representations is maximized [2]. However, PCA is not appropriate for nonlinear features, because it is employed in a linear way. Alternatively, manifold learning techniques can map nonlinear high-dimensional data to low-dimensional space [3], [4]. Manifold learning techniques assume that the data of interest lies on an embedded non-linear manifold within the high-dimensional space while preserving neighborhood relations between nearest neighbors. Therefore, they can perform nonlinear dimensionality reduction by applying embedding to high-dimensional features.

In the remainder of this paper, we describe our disease classification approach, which first extracts morphological features from short-axis cine MRI of a subject by finding the spatial transformation that places the scan into a common space. We then compute the Jacobian determinants of the transformations which we relate to tissue density maps. The Jacobian determinants are then embedded into a lower-dimensional space via manifold learning. We then use the resulting embedding coordinates as the lower-dimensional features for disease detection. The method is applied to MRI scans of 12 normal controls and 22 tetralogy of Fallot patients and evaluated by classification rates using leave-one-out method.

2 Method

Fig. 1 summarizes our morphological classification framework. We first extract morphological features for each subject from the given ventricular segmentations of patients' medical scan image. We then use the morphological features to learn a low-dimensional embedding via a manifold learning technique targeted towards dimensionality reduction. Each scan is now represented by coordinates in the low-dimensional embedding. We then apply these coordinates to a non-linear support vector machine classifier to produce the class label. In followings, we will explain each component in detail.

2.1 Feature Extraction

We use the RAVENS maps as a morphological descriptor characterizing the images [5]. RAVENS maps are the results of deformable registration of cardiac images to a common template while generating maps that are proportional to each individual's regional tissue amount. They capture tissue density, which tetralogy of Fallot patients often affect.

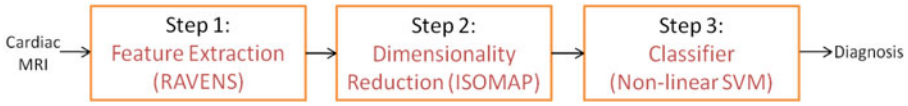

Fig. 1. Overview of proposed framework

Suppose S_k denotes the segmented image for tissue k in the individual image $S : \Omega_S \to \mathbf{R}$ and $T : \Omega_T \to \mathbf{R}$ is the template to be registered. Then a RAVENS map, $\mathcal{D}_k : \Omega_T \to \Omega_T$, for tissue k is defined as:

$$\mathcal{D}_k(x) := J(h(x))S_k(h(x))$$

with h being the deformation map from Ω_S to Ω_T and $J(h(x))$ is the Jacobian determinant of h at voxel x.

We create the RAVENS map, by registering the images to the common atlas via fast diffeomorphic demons algorithm [6]. When registering the images, the choice of a template plays an important role in the accuracy of the morphological features. Therefore, it is necessary to select the optimal template for better morphological representations. In order to select the optimal template, we adopt GRAM framework [7] which finds the geodesic mean of the data. GRAM computes the geodesic distance between two images by viewing the dataset as undirected graph with the nodes of the graph representing the images of the data set. $g(I_i, I_j)$, the geodesic distance between two images I_i and I_j, is approximated by the shortest path between the two corresponding nodes in the graph. The geodesic mean template T is then defined by the image in the data set with minimum distance to all other images:

$$T = \arg\min_i \sum_j g(I_i, I_j).$$

After registering all images to T, we reduce the noise in the RAVENS maps via Gaussian kernel smoothing. We further reduce the number of features by only using the RAVENS map $\mathcal{D}_{RV}$ of the right ventricle for classification. We do so because right ventricle is the most significant tissue type related to Tetralogy of Fallot.

2.2 Dimensionality Reduction

Even after confining the RAVENS maps to the right ventricle, its dimensionality is still very high compared to the limited sample size. As mentioned, this generally negatively influences the accuracy of the classifier. We address the issue by performing dimensionality reduction via the ISOMAP algorithm [4].

In order to apply the ISOMAP algorithm, we represent the data as a graph whose vertex corresponds to the image samples. First, we define the edge length $d(i, j)$ between two subjects i and j as a $L2$ distance of RAVENS maps:

$$d(i, j) := \sum_{x \in \Omega_T} (\mathcal{D}^i_{RV}(x) - \mathcal{D}^j_{RV}(x))^2,$$

We then construct a connected k-NN graph based on the edge lengths $d(i, j)$. We then use the k-NN graph to infer the geodesics between all pairs of subjects. This results are stored in a matrix with the size corresponding to the number of samples. We then generate the low-dimensional embedding of the data by computing the eigenvalues and -vectors of the matrix. The eigenvectors of the 9 highest eigenvalues then define the coordinate system of the low-dimensional embedding of the data set. Finally, each data set is described by its (embedding) coordinates in that coordinate system. By doing so, we reduced the number of features describing each data set from 172800 to 9.

2.3 Non-linear SVM

The embedding coordinates of each image are fed into classifier, which labels each data set based on those features. We choose the support vector machine (SVM) classifier [8] for this task. SVM is a popular approach pattern classification. It separates the data into two clusters hopefully representing the healthy and diseased population. This separation is described through a hyperplane. The hyperplane is generated by training the algorithm on a pre-classified training set. From this training set, the algorithm selects a relatively small number of samples that are close to the opposite group. These samples are called support vectors and are used for defining the dividing hyperplane. By doing so, the classifier inherently focuses on the subtleties of the morphological differences between normal controls and tetralogy of Fallot patients and not on data sets that are easy to detect.

While the SVM classifier is very effective in finding this hyperplane, selecting the type of hyperplane is very important. If the hyperplane is too stiff then the algorithm might not perfectly separate the two groups. On the other hand, if the hyperplane is too flexible then the algorithm will overfit the data. The type of hyperplane is characterized by the kernel that maps the data to a higher-dimensional where linear separation is possible. Based on our experience, we choose the Gaussian radial basis function as kernel [9].

$$K(u, v) := exp(-\gamma||u - v||^2),$$

where u and v are data points and γ is a model parameter.

In summary, we conduct supervised classification with embedding coordinates on the cardiac MRI scans of 34 subjects. In our application, we consider tetralogy of Fallot as a positive data, and normal controls as a negative data. We choose the support vector machine with radial basis function kernel as a classifier due to its effectiveness and efficiency. The classifier is trained on the 33 subjects and trained classifier was applied to the 1 left-out data. We select the model parameter γ in the radial basis function by grid search using cross validation.

3 Experiment

We evaluate our method by applying it on short-axis cardiac MRIs of 12 normal volunteers and 22 Tetralogy of Fallot patients. Tetralogy of Fallot patients

were post-repaired and age-matched to normal controls. Steady-state free precession cardiac MRIs were obtained at end-diastole. The acquired short-axis slice covered the whole heart. To prevent other organs from influencing analysis, the images were cropped using manually defined rectangular regions that enclosed the complete left ventricle and right ventricle on the short axis, respectively. The left ventricular endocardium, left ventricular epicardium, and right ventricular epicardium were semi-automatically segmented in the data set on short-axis slices [10]. We then applied the data set to our pipeline. We measuring the accuracy of our approach via leave-one-out cross validation comparing the classification of the test subject with the diagnosis of an expert. For comparison, we also computed the accuracy of the non-linear SVM classifier using the left and right ventricular volume as input features.

3.1 Features

Fig. 2 shows the distribution of the features used as input to the SVM classifier. Fig. 2a plots the left and right ventricular volume features and Fig. 2b shows the two-dimensional embedding of RAVENS map. It is worth to mentioning that for classification of the RAVENS map we actually used 9 dimensional features. However, it is practically impossible to visualize 9 dimensional features. Therefore, we confine our low-dimensional embedding to the first two largest eigenvalues for visualization purpose. A subset of images is also shown with embedding in Fig. 2b. The embedding conveniently summarizes the change in right ventricle size as the most dominant parameter. These type of observation support the impression that neighborhoods in the embedding coordinates represent images that are similar in terms of the size of right ventricle. Furthermore, we note that ventricular volume features have more overlap between normal controls and tetralogy of fallots in the feature space than embedding coordinates. Therefore, embedding coordinates can have more discriminative power than ventricular volume features. In addition, distribution of embedding coordinates is not linearly separable. This indicates that non-linear kernel mapping is necessary for these features.

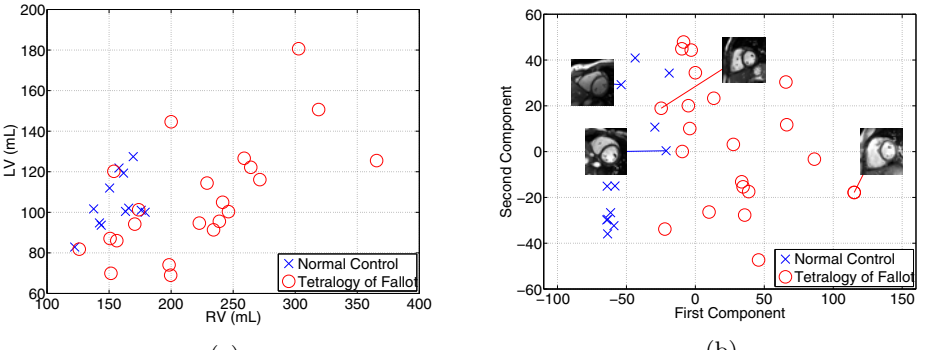

(a) (b)

Fig. 2. Feature distribution (a) Ventricle volume (b) 2D ISOMAP of RAVENS maps

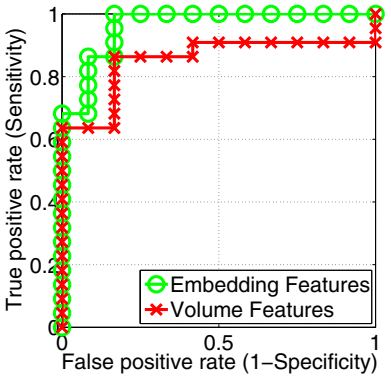

Fig. 3. Receiver Operating Characteristics(ROC) curves for embedding features and ventricular volumetric features

Table 1. Recall rates between Normal Control versus Tetralogy of Fallot

	Sensitivity(%)	Specificity(%)	AUC(%)
Ventricular volumes	86.36	75	85.2
Embedding coordinates	**95.45**	**83.33**	**96.4**

3.2 Classification Accuracy

The classification performance was measured by precision recall rate. In the binary classification of positive tetralogy of fallot and negative normal hearts, the results are represented by numbers of true positive(TP), false positive(FP), true negative(TN), and false negative(FN). The sensitivity and specificity were computed by

$$sensitivity = \frac{TP}{TP + FN}, specificity = \frac{TN}{TN + FP}$$

In addition, area under the curves (AUC) are computed by ROC analysis in Fig. 3. Table 1 shows precision recall rates and AUC for ventricular volume features and embedding coordinates. Compared to ventricular volume features, embedding coordinates achieves higher sensitivity (10.09% increase), specificity (11.07% increase) and AUC (11.2% increase). This result indicates that the features generated by ISOMAP applied to the RAVENS maps better characterize the disease compared to ventricular volume features often used in the clinical setting.

3.3 Group Comparisons via Voxel-Based Analysis

Although nonlinear classification methods are generally effective in resolving spatially complex group differences, they do not easily lend themselves to intuitive interpretation of the result. For clinical evaluation, we need to identify

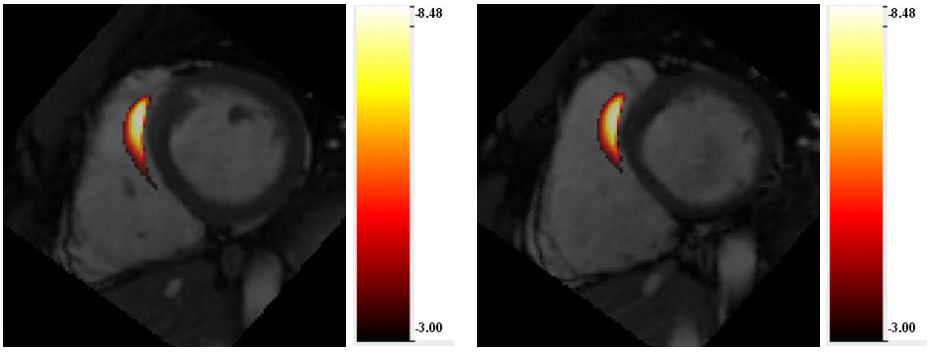

Fig. 4. Maps of the t statistics showing differences between normal controls and tetralogy of fallot patients. T-maps are presented in different mid slices of the cropped template image. Regions in which tetralogy of fallot patients are significantly different from normal controls are highlighted in red, reflecting right ventricular outflow tract (RVOT) obstruction. T-maps were thresholded at the $p = 0.001$ level. Color bar represents logarithm of p value.

abnormalities such as progressive hypertrophy and chamber dilation. However, the high dimensional features are generally not displayable in a single image. We thus choose an alternative approach called voxel-based group comparisons to visualize the differences between healthy and diseased subjects [11]. Fig. 4 shows the t-statistics thresholded at $p = 0.001$ level in different mid slices. This figure shows significant right ventricular shape changes in tetralogy of fallot compared to healthy hearts. Right ventricular outflow tract, which are generally implicated in tetralogy of fallot, are highlighted (red color). This implies that our classification method can precisely localize the region of pathology in tetralogy of fallot patients compared to normal subjects.

4 Conclusion

We presented a disease classification frame work to diagnose tetralogy of Fallot patients. Mass-preserving morphological descriptors were used to extract morphological features from cardiac MRI. We then reduced the dimensionality of features via ISOMAP. The reduced features were fed into the non-liner support vector machine classifier to produce labellings of healthy and diseased patient group. On a small data set, classification based on our features outperformed conventional clinical analysis based on the volume of the ventricle. We believe this improved performance was due to better morphological descriptors and non-linear classifier.

Acknowledgment. The research was supported by an ARRA supplement to NIH NCRR (P41 RR13218).

References

1. Helbing, W.A., Roos, A.: Clinical application of cardiac magnetic resonance imaging after repair of tetralogy of Fallot. Pediatric Cardiology 21(1), 70–79 (2000)
2. Sirovich, L., Kirby, M.: Low-dimensional procedure for the characterization of human faces. Journal of the Optical Society of America A(4), 519–524 (1987)
3. Roweis, S., Saul, L.: Nonlinear Dimensionality Reduction b Locally Linear Embedding. Science 290, 2323–2326 (2000)
4. Tenenbaum, J.B., Silva, V., Langford, J.C.: A Global Geometric Framework for Nonlinear Dimensionality Reduction. Science 290(5500), 2319–2323 (2000)
5. Davatzikos, C., Genc, A., Xu, D., Resnick, S.M.: Voxel-based morphometry using the ravens maps: methods and validation using simulated longitudinal atrophy. Neuroimage 14(6), 1361–1369 (2001)
6. Vercauteren, T., Pennec, X., Perchant, A., Ayache, N.: Diffeomorphic demons: efficient non-parametric image registration. Neuroimage 45(supp.1), S61–S72 (2009)
7. Hamm, J., Ye, D.H., Verma, R., Davatzikos, C.: Gram: A framework for geodesic registration on anatomical manifolds. Med. Image Anal. 14(5), 633–642 (2010)
8. Burges, C.J.C.: A tutorial on support vector machines for pattern recognition. Data Mining and Knowledge Discovery 2, 121–167 (1998)
9. Keerthi, S., Lin, C.: Asymptotic behaviors of support vector machines with Gaussian kernel. Neural Computation 15(7), 1667–1689 (2003)
10. Heiberg, E., Wigstrom, L., Carlsson, M., Bolger, A.: Time Resolved Treedimensional Automated Segmentation of the Left Ventricle. Proceedings of IEEE Computers in Cardiology 32, 599–602 (2005)
11. Ashburner, J., Friston, K.J.: Voxel-based morphometry–the methods. Neuroimage 11(6 Pt 1), 805–821 (2000)